Applied Physics A

Impact of annealing on martensitic transformation of Mn50Ni42.5Sn7.5 shape memory alloy

--Manuscript Draft--

Manuscript Number:	APYA-D-18-01762R1
Full Title:	Impact of annealing on martensitic transformation of Mn50Ni42.5Sn7.5 shape memory alloy
Article Type:	Regular papers
Corresponding Author:	Tarek Bachaga, Ph.D. Universite de Sfax Faculte des Sciences de Sfax TUNISIA
Corresponding Author Secondary Information:	
Corresponding Author's Institution:	Universite de Sfax Faculte des Sciences de Sfax
Corresponding Author's Secondary Institution:	
First Author:	Tarek Bachaga, Ph.D.
First Author Secondary Information:	
Order of Authors:	Tarek Bachaga, Ph.D.
	J. Zhang
	S Ali
	J.J. Sunol
	M. Khitouni
Order of Authors Secondary Information:	
Funding Information:	
Abstract:	The impact of annealing on the structural and martensitic transformation of Mn50Ni42.5Sn7.5 (at.%) shape memory alloy was systematically investigated using a scanning electron microscope (SEM), X-ray diffraction (XRD), and differential scanning calorimetry (DSC). According to XRD studies, martensite phase a 14M modulated monoclinic structure was detected, at room temperature, for as-cast and annealed alloys. In addition, it has observed that during annealing, the transition temperatures have increased relative to the cast alloy. Also, a high dependence between the cooling rate and activation energy has detected. The more detailed characterization of martensitic transition and account of thermodynamic parameters were examined after annealing.
Response to Reviewers:	Dear Sir, At first, I would like to thank the reviewer 1 for the constructive remarks and the interest discussions offer for our paper. The given questions pushed us to make another bibliography and discovered the interesting result deduced from the effect of annealing condition on martensitic transformation in a Mn-Ni-Sn alloy. We have considered all your suggestions, which are corrected in the manuscript as following: Responses for Reviewer 1 Comments Question 1: "English text is generally well written using straightforward expressions. However, there is occasional carelessness noticeable in the manuscript and they are better to be corrected by proof reading of the native English speaker." Response Thank you for your comment. The English language has been improved. Question 2: “Page 3, line 4; As you know, vapor pressure of Mn is very high and arc remelting of pure Mn might be very difficult. What was your plan for recycling Mn and control the composition? Meanwhile, evaporation of Mn and its deposition on the visor of the furnace could be another problem. Please explain in detail how did you perform

	the melting process?" Response Yes, you are right, we detailed the melting process. The equipment used in this study is the Compact Arc Melter MAM-1 model of the commercial house Edmund Bühler. The precursors used to obtain the Mn50Ni42.5Sn7.5 (at. %) bulk alloy are: a Ni metal filament (purity> 99.98%), metallic manganese sheets (purity> 99.98%) and pieces of metallic Sn in the form of small spheres (purity> 99.99%). An extra 5 wt.% Mn was added to compensate for evaporation losses. Polycrystalline of about 4g were prepared by the melting of the precursors under argon atmosphere in a water-cooled copper crucible. The bulk alloy was melted four times, to ensure the homogeneity of the chemical composition. In our case, the starting elements have a high melting point, such as: Melting point of Ni= 1455C, Mn= 1246C, Sn= 231C. To better ensure the recycling of the Mn and control the composition, the elements were placed increasingly according to their melting temperatures more precisely the Sn and the Mn finally the highest Ni. The bulk alloy was fixed in a quartz tube filled with argon gas followed by annealing at 1273 K for 1h, and then quenched in ice water. Page 3, L4-14: " An as-cast ingot with a nominal composition of Mn50Ni42.5Sn7.5 (at. %) was prepared by arc melting from a Ni metal filament (purity> 99.98%), metallic manganese sheets (purity> 99.98%) and pieces of metallic Sn in the form of small spheres (purity> 99.99%), using Buhler MAM-1 compact arc melting under an argon atmosphere. The mass of the ingot prepared by arc melting was 4 g. An extra 5 wt.% Mn was added to compensate for evaporation losses. The bulk alloy was melted four times, to ensure the homogeneity of the chemical composition. In our case, to better ensure the recycling of the Mn and control the composition, the elements were placed increasingly according to their melting temperatures more precisely the Sn (Tf=231 C) the lowest and the Mn (Tf=1246 C) finally the highest Ni (Tf=1455 C). The bulk alloy was fixed in a quartz tube filled with argon gas, followed by annealing at 1273 K for 1h, and then quenched in ice water". Question 3: "Page 3, line 19; Did you measure the mean grain size?" Response Yes, thank you for this comment. The mean grain size was measured from SEM images of as-cast and annealed samples by image J software. "ImageJ has a diverse user community and due to the wide range of possible applications, can be daunting; there is a lot of information and plugins out there. Some users may want to explore the amazing diversity of options eventually, but it is not necessary to get started. By focusing only on the things needed for particle analysis, you can be analyzing scanned images within 15 minutes of downloading". http://www.smalldropsprays.info/stepbystepmethods/ImageJ-software https://www.youtube.com/watch?v=YPQsCjHzWg4 Page 3, L18-19: “The mean grain size was measured from SEM images of as-cast and annealed samples by image J software". Question 4: "Page 3, line 24; EDX is a semi-quantified analysis and is not reliable for composition control." Response Yes, you are right; EDX is a semi-quantitative analysis sufficient only to recognize the different phases. But, in our work, we must to know the composition of our samples with an error of 0.3-0.6% element by element, so we have passed the quantitative analysis with standards. Page 4, L7-9: "The standard deviation obtained for the elemental chemical composition (as determined by EDX) was 0.4–0.6 at% for Mn, 0.4–0.6 at% for Ni, and 0.3–0.5 at% for Sn". Question 5: "Page 4, line 1; what is the "mixed metallic elements”?! Metallic compound? Is this a result?" Response Yes, you are right; in our case, the bulk alloy was melted four several times, to ensure the homogeneity of the chemical composition. The EDX analysis of the as-cast and annealed samples confirms the presence of the metallic mixture. Page 4, L9-14: " The EDX analysis of the as-cast and annealed samples is shown in Figure 1(a2) and 1(b2). The results confirm the presence of the metallic mixture. The compositions analysis was found to be in good agreement with the nominal compositions of the as-cast and annealed samples ((49.88 at.% Mn-42.69 at.% Ni-7.43 at.% Sn) and (49.33 at.% Mn-43.22 at.% Ni-7.45 at.% Sn)). The compositions are shifted from the original. It is usual in these alloys obtained by arc melting followed by annealing".

Question 6: Page 5, line 3; Please rewrite this sentence: "This expansion in the estimation related to the variation of the composition may be due to the volatilization of some Manganese during the annealing treatment."
Response
Thanks for the comments. The sentence has been rewritten:
Page 5, L12-14: "They showed that all these progression temperatures increase with the ratio (e/a). The values of this report in our work are 8.05 and 8.07, respectively. This increase in (e/a) values may be due to the volatilization of some Manganese during annealing."
Question 7: Page 5, line 10; which parameter of annealing did you mean? Temperature? Time?
Response
Thanks for your valuable comment. We have noted the annealing parameter corresponding to the theoretical basis of the martensitic transformation in the following text:
Page 6, L1-3: "The last parameter is the main parameter must be obtained, to get the kinetic transformation of the both alloys. The Kissinger method for non-isothermal change was used to obtain the activation energy. In this case, the temperature of the peak T is utilized to decide the activation energy of two changes since, it has examined that the change was isokinetic ".
Question 8: Page 6, line 10; What is the importance of critical points? You should explain more about your final result.
Response
Thanks for this professional suggestion. The details have been added to the revised manuscript.
Pages 7-8: "Figure 5 shows the plot of Ln(β/T2) versus 1/T. The values of the activation energy Ea for the annealed alloy were determined by the slope of the Ln(β/T2) versus 1/T curves. It is clear that there is a remarkable difference in activation energy for various scanning rates. The calculated values Ea are: 259.604 and 12.215 kJ.mol-1, respectively. This difference in Ea leads to a dependence of the cooling rate and the activation energy Ea, where the high cooling rates and the low cooling rates correspond to very different activation energies. Meanwhile, over a wide range of rates (5 to 10 °C.min-1) between the both previous activation energies, the high values can slowly change to low values. This enables us to deduce that the critical point position 8 °C.min-1, as shown in Figure 5. The kinetics of other alloys with first-order martensitic transformation, for example Cu-Ni-Al [26], Fe-C(N) [27] and Ti–Al–V [28], as well as the ordering transition kinetics in Ni-Mn-Ga [29] have also been widely determined using Kissinger method [30], based on colorimetric results. While, scaling rates are greater than 5°C.min-1 in the aforementioned literature, limited work has been limited on the rate dependence of activation energy at lower speeds. Fernandez et al. [31] have shown that there seems to be, by all accounts, a critical point related to the slope of the linear curves of Ln(β/T2) with respect to 1/T, and attributed this phenomenon to evaluated error. In the study of the Ni-Ti shape memory alloy, Hsu et al. [32] have reported that the martensitic substructure could move from coarse twins to fine twins or stacking defects with cooling rates varying from 0.5 to 25 K.min-1. In addition, the atomic displacement of the stacking defects in the surface (0 0 1) with a high cooling rate is only a large part of that with a lower cooling rate. Accordingly, the purpose behind the rate dependence of activation energy in the present investigation could likely be identified with the way that twinning and atomic displacements in the martensitic change process increase significantly at generally low cooling rates, which causes an increase in activation energy important for the progress. The speed of stage interfaces relies upon just the undercooling as the temperature rate abatements to low values [33]. Thusly, fast sample cooling would support a bigger undercooling in a generally short time in examination with cooling gradually, which is in charge of a bigger chemical driving force, and therefore for lower activation energy."
[26] V. Recarte, J.I. Perez-Landazabal, A. Ibarra, M.L. No, J.S. Juan. High temperature β phase decomposition process in a Cu-Al-Ni shape memory alloy. Mater. Sci. Eng. A 378, 238-242 (2004)
[27] Z. Guo, W. Sha, D. Li. Quantification of phase transformation kinetics of 18 wt.% Ni C250 maraging steel. Mater. Sci. Eng. A 373, 10-20 (2004)
[28] S. Malinov, Z. Guo, W. Sha, A. Wilson. Differential scanning calorimetry study and computer modeling of β→α phase transformation in a Ti-6Al-4V alloy. Metall. Mater. Trans. A 32, 879-887 (2001)
[29] V Sanchez-Alarcos, J.I. Perez-Landazabal, V. Recarte, J.A. Rodrıguez-

Velamazan, V.A. Chernenko. J. Phys: Condens. Matter 22, 166001 (2010)
[30] J. Vazquez, P. Villares, R. Jimenez-Garay. A theoretical method for deducing the evolution with time of the fraction crystallized and obtaining the kinetic parameters by DSC, using non-isothermal techniques. J. Alloy. Compd 257, 259 (1997)
[31] J. Fernandez, A.V. Benedetti, J.M. Guilemany, X.M. Zhang. Thermal stability of the martensitic transformation of Cu-Al-Ni-Mn-Ti. Mat. Sci. Eng. A 438-440, 723-725 (2006)
[32] T.Y. Hsu. Martensitic transformation and martensite. Beijing: Science (1999)
[33] Z.Q. Kuang, J.X. Zhang, X.H. Zhang, K.F. Liang, P.C.W. Fung. Scaling behaviours in the thermoelastic martensitic transformation of Co. Solid. State. Commun 114, 231-235 (2000)
General remarks/
-References are also added ([26-33]).
-The quality of all figures has been improved.
Sincerely Yours.
Dr. T BACHAGA

Dear Sir,
At first, I would like to thank the reviewer 2 for the constructive remarks and the interest discussions offer for our paper. The given questions pushed us to make another bibliography and discovered the interesting result deduced from the effect of annealing condition on martensitic transition of Heusler Mn50Ni42.5Sn7.5 alloy. We have considered all your suggestions, which are corrected in the manuscript as following:
Responses for Reviewer 2 Comments
Question 1: "The paper is reasonably written, headline is o.k. The language needs improvement by native speaker."
Response
Thank you for your comment. The English language has been improved.
Question 2: "The figures are rather poor in quality in the present manuscript. Should be delivered in better quality if possible."
Response
Yes, you are right. The quality of all figures has been improved.
Question 3: "The only critical scientific point is the Kissinger analysis of DSC data. Fig. 5 shows two ranges, 2 and 5K/min and the data 10K/min and higher heating rate. Corresponding activation energies differ largely. However, if one looks into the original DSC Data fig. 4 it is obvious, that measurements at intermediate heating rates show no single peak, but double hump like structure. Thus, two transformations occur nearly simultaneously. Thus the Kissinger analysis is not directly applicable. Authors need to check and discuss this."
Response
Thank you for this professional suggestion. Yes, you are right, if we look at the original DSC data (Figure 4), it is obvious that the measurements at intermediate cooling rates show no single peak, but a double-hump structure. What is unique in our study of the Mn50Ni42.5Sn7.5 sample is that two exothermic peaks can be observed during the intermediate cooling rates. Previous studies had never reported such an abnormal phenomenon. They proposed that, in addition to martensitic transformation, another inter-martensitic transformation takes place between two martensitic phases of different structures. Thus, it is reasonable to consider the current transformation peaks in the DSC curve of the Mn50Ni42.5Sn7.5 sample as a martensitic transformation and an inter-martensitic transformation, which are completely reversible and reproducible. Furthermore, the purpose of calculating the activation energy is to determine level of energy required by the sample as the martensite transformation takes place, which indicates how stable a structure is displayed by alloy. The Johnson–Mehl–Avrami (JMA) equation for solid state transformation can be used to determine activation energy of shape memory alloys when phase transformations occur. The JMA equation can be applied non-isothermal case. The Kissinger method is proposed for analyzing non-isothermal activation energy of samples. The details have been added to the revised manuscript.
Pages 6-8: “From measurements obtained by DSC, we can examine the theory of martensitic transformation; specifically the activation energy Ea. The last parameter is the main parameter must be obtained, to get the kinetic transformation of the both alloys. The Kissinger method for non-isothermal change was used to obtain the activation energy. In this case, the temperature of the peak T is utilized to decide the

activation energy of two changes since, it has examined that the change was isokinetic.
Distinctive cooling rates running from 2 to 50 °C.min-1 were used to make these measurements. Figure 4 shows the thermograms acquired for various cooling rates. It is clear that the transition temperatures decrease with increasing cooling rates and the progress temperatures extend demonstrates a propensity to widen with expanding cooling rate. Moreover, what is unique in our investigation of the Mn50Ni42.5Sn7.5 sample is that two exothermic peaks can be observed during intermediate cooling rates. Previous studies had never detailed such an abnormal phenomenon [23, 24]. They proposed that, in addition to martensitic transformation, another inter-martensitic transformation happens between two martensitic phases of various structures. In this way, it is reasonable to consider the current transformation peaks in the DSC curve of the Mn50Ni42.5Sn7.5 sample as a martensitic transformation and an inter-martensitic transformation, which are completely reversible and reproducible. According to the data obtained from the DSC curve, the peaks temperatures of the inter-martensitic transformations during cooling intermediate cooling rates 10 and 20C.min-1 are 393 and 391 K, respectively. The thermal activation energies of samples were carried out by DSC with different cooling rates as 2, 5, 10, 20, 30 and 50 °C.min-1 (Figure 4). The purpose of calculating the activation energy is to determine level of energy required by the sample during martensitic transformation. The Johnson–Mehl–Avrami (JMA) equation for solid state transformation can be used to determine the activation energy of shape memory alloys as phase transformations occur. The JMA equation can be applied non-isothermal case. The Kissinger method is proposed for the analysis of non-isothermal activation energy of samples [25]. From JMA, the fraction X of the SMAs after a given time t was indicated by the following equation:
$X=1-\exp[-(Kt)n]$
(1)
Where n is the Avrami exponent and K is the effective reaction rate usually assigned Arrhenius temperature dependence:
$K=Ko\exp(-Ea/RT)$
(2)
The Kissinger method is a one solution of Arrhenius equation. The activation energy can be calculated by applying the following equation according to the Kissinger method.
$Ln(\beta/T2)=A-Ea/RT$
(3)
Where Ea is the activation energy, T is the maximum peak temperature of transition, R is the gas constant (8.314 J.mol-1), β is the cooling rate and A is the constant coefficient. Figure 5 shows the plot of Ln(β/T2) versus 1/T. The values of the activation energy Ea for the annealed alloy were obtained from the slope of the line obtained by plotting Ln(β/T2) versus 1/T. It is clear that there is a remarkable difference in activation energy for various scanning rates. The calculated values Ea are: 259.604 and 12.215 kJ.mol-1, respectively. This difference in Ea leads to a dependence of the cooling rate and the activation energy Ea, where the high cooling rates and the low cooling rates correspond to very different activation energies. Meanwhile, over a wide range of rates (5 to 10 °C.min-1) between the both previous activation energies, the high values can slowly change to low values. This enables us to deduce that the critical point position 8 °C.min-1, as shown in Figure 5. The kinetics of other alloys with first-order martensitic transformation, for example Cu-Ni-Al [26], Fe-C(N) [27] and Ti-Al-V [28], as well as the ordering transition kinetics in the Ni-Mn-Ga alloy [29] were largely determined using Kissinger method [30], based on colorimetric results. While, scaling rates are greater than 5°C.min-1 in the previously mentioned literature, limited work has been limited on the rate dependence of activation energy at lower speeds. Fernandez et al. [31] have shown that there seems to be, by all accounts, a critical point related to the slope of the linear curves of Ln(β/T2) with respect to 1/T, and attributed this phenomenon to evaluated error. In the investigation of the Ni-Ti shape memory alloy, Hsu et al. [32] reported that the martensitic substructure could move from coarse twins to fine twins or stacking defects with cooling rates changing from 0.5 to 25 K.min-1. In addition, the atomic displacement of the stacking defects in the surface (0 0 1) with a high cooling rate is just a large part of that with a lower cooling rate. Therefore, the reason behind the rate dependence of activation energy in the present examination could probably be identified with the way that twinning and atomic displacements in the martensitic transformation process increase significantly at generally low cooling rates, which causes an increase in activation energy important

	for the progress. The speed of stage interfaces relies upon just the under-cooling as the temperature rate reductions to low values [33]. Thus, the rapid cooling of the samples would promote greater under-cooling in a generally short time during an examination with progressive cooling, which is responsible for a larger chemical driving force, and therefore lower activation energy. In this way, an example of rapid cooling would reinforce greater under-cooling in a relatively short examination time, with step cooling, which is responsible for a greater synthetic main thrust, and along these lines for lower initiation vitality ''. [23] H.X. Zheng, M.X. Xia, J. Liu, J.G. Li. Martensitic transformation of highly undercooled Ni-Fe-Ga magnetic shape memory alloys. J. Alloy. Compd 385, 144 (2004) [24] H.X. Zheng, J. Liu, M.X. Xia, J.G. Li. Martensitic transformation of Ni-Fe-Ga magnetic shape memory alloys. J. Alloy. Compd 387, 265 (2005) [25] H. Fang, B. Wong, Y. Bai. Kinetic modelling of thermophysical properties of shape memory alloys during phase transformation. Const. Buil. Mater 131, 146–155 (2017) [26] V. Recarte, J.I. Perez-Landazabal, A. Ibarra, M.L. No, J.S. Juan. High temperature β phase decomposition process in a Cu-Al-Ni shape memory alloy. Mater. Sci. Eng. A 378, 238-242 (2004) [27] Z. Guo, W. Sha, D. Li. Quantification of phase transformation kinetics of 18 wt.% Ni C250 maraging steel. Mater. Sci. Eng. A 373, 10-20 (2004) [28] S. Malinov, Z. Guo, W. Sha, A. Wilson. Differential scanning calorimetry study and computer modeling of β→α phase transformation in a Ti-6Al-4V alloy. Metall. Mater. Trans. A 32, 879-887 (2001) [29] V Sanchez-Alarcos, J.I. Perez-Landazabal, V. Recarte, J.A. Rodrıguez-Velamazan, V.A. Chernenko. J. Phys: Condens. Matter 22, 166001 (2010) [30] J. Vazquez, P. Villares, R. Jimenez-Garay. A theoretical method for deducing the evolution with time of the fraction crystallized and obtaining the kinetic parameters by DSC, using non-isothermal techniques. J. Alloy. Compd 257, 259 (1997) [31] J. Fernandez, A.V. Benedetti, J.M. Guilemany, X.M. Zhang. Thermal stability of the martensitic transformation of Cu-Al-Ni-Mn-Ti. Mat. Sci. Eng. A 438-440, 723-725 (2006) [32] T.Y. Hsu. Martensitic transformation and martensite. Beijing: Science (1999) [33] Z.Q. Kuang, J.X. Zhang, X.H. Zhang, K.F. Liang, P.C.W. Fung. Scaling behaviours in the thermoelastic martensitic transformation of Co. Solid. State. Commun 114, 231-235 (2000) Sincerely Yours. Dr. T BACHAGA General remarks/ -References are also added ([26-33]). -The quality of all figures has been improved.

Dear Sir,

At first, I would like to thank the reviewer for the constructive remarks and the interest discussions offer for our paper. The given questions pushed us to make another bibliography and discovered the interesting result deduced from the effect of annealing condition on martensitic transformation in a Mn-Ni-Sn alloy. We have considered all your suggestions, which are corrected in the manuscript as following:

Responses for Reviewer 1 Comments

Question 1: "English text is generally well written using straightforward expressions. However, there is occasional carelessness noticeable in the manuscript and they are better to be corrected by proof reading of the native English speaker."

➲ **Response**

Thank you for your comment. The English language has been improved.

Question 2: "Page 3, line 4; As you know, vapor pressure of Mn is very high and arc remelting of pure Mn might be very difficult. What was your plan for recycling Mn and control the composition? Meanwhile, evaporation of Mn and its deposition on the visor of the furnace could be another problem. Please explain in detail how did you perform the melting process?"

➲ **Response**

Yes, you are right, we detailed the melting process. The equipment used in this study is the Compact Arc Melter MAM-1 model of the commercial house Edmund Bühler. The precursors used to obtain the $Mn_{50}Ni_{42.5}Sn_{7.5}$ (at. %) bulk alloy are: a Ni metal filament (purity> 99.98%), metallic manganese sheets (purity> 99.98%) and pieces of metallic Sn in the form of small spheres (purity> 99.99%). An extra 5 wt.% Mn was added to compensate for evaporation losses. Polycrystalline of about 4g were prepared by the melting of the precursors under argon atmosphere in a water-cooled copper crucible. The bulk alloy was melted four times, to ensure the homogeneity of the chemical composition. In our case, the starting elements have a high melting point, such as: Melting point of Ni= 1455°C, Mn= 1246°C, Sn= 231°C. To better ensure the recycling of the Mn and control the composition, the elements were placed increasingly according to their melting temperatures more precisely the Sn and the Mn finally the highest Ni. The bulk alloy was fixed in a quartz tube filled with argon gas followed by annealing at 1273 K for 1h, and then quenched in ice water.

Page 3, L4-14: " An as-cast ingot with a nominal composition of $Mn_{50}Ni_{42.5}Sn_{7.5}$ (at. %) was prepared by arc melting from a Ni metal filament (purity> 99.98%), metallic manganese sheets (purity> 99.98%) and pieces of metallic Sn in the form of small spheres (purity> 99.99%), using Buhler MAM-1 compact arc melting under an argon atmosphere. The mass of the ingot prepared by arc melting was ~ 4 g. An extra 5 wt.% Mn was added to compensate for evaporation losses. The bulk alloy was melted four times, to ensure the homogeneity of

the chemical composition. In our case, to better ensure the recycling of the Mn and control the composition, the elements were placed increasingly according to their melting temperatures more precisely the Sn (T_f=231 °C) the lowest and the Mn (T_f=1246 °C) finally the highest Ni (T_f=1455 °C). The bulk alloy was fixed in a quartz tube filled with argon gas, followed by annealing at 1273 K for 1h, and then quenched in ice water".

Question 3: "Page 3, line 19; Did you measure the mean grain size?"

➲ **Response**

Yes, thank you for this comment. The mean grain size was measured from SEM images of as-cast and annealed samples by image J software. "ImageJ has a diverse user community and due to the wide range of possible applications, can be daunting; there is a lot of information and plugins out there. Some users may want to explore the amazing diversity of options eventually, but it is not necessary to get started. By focusing only on the things needed for particle analysis, you can be analyzing scanned images within 15 minutes of downloading".

http://www.smalldropsprays.info/stepbystepmethods/ImageJ-software

https://www.youtube.com/watch?v=YPQsCjHzWg4

Page 3, L18-19: "The mean grain size was measured from SEM images of as-cast and annealed samples by image J software".

Question 4: "Page 3, line 24; EDX is a semi-quantified analysis and is not reliable for composition control."

➲ **Response**

Yes, you are right; EDX is a semi-quantitative analysis sufficient only to recognize the different phases. But, in our work, we must to know the composition of our samples with an error of 0.3-0.6% element by element, so we have passed the quantitative analysis with standards.

Page 4, L7-9: "The standard deviation obtained for the elemental chemical composition (as determined by EDX) was 0.4–0.6 at% for Mn, 0.4–0.6 at% for Ni, and 0.3–0.5 at% for Sn".

Question 5: "Page 4, line 1; what is the "mixed metallic elements"?! Metallic compound? Is this a result?"

➲ **Response**

Yes, you are right; in our case, the bulk alloy was melted four several times, to ensure the homogeneity of the chemical composition. The EDX analysis of the as-cast and annealed samples confirms the presence of the metallic mixture.

Page 4, L9-14: " The EDX analysis of the as-cast and annealed samples is shown in Figure 1(a2) and 1(b2). The results confirm the presence of the metallic mixture. The compositions analysis was found to be in good agreement with the nominal compositions of the as-cast and annealed samples ((49.88 at.% Mn-42.69 at.% Ni-7.43 at.% Sn) and (49.33 at.% Mn-43.22 at.% Ni-7.45 at.% Sn)). The compositions are shifted from the original. It is usual in these alloys obtained by arc melting followed by annealing".

Question 6: Page 5, line 3; Please rewrite this sentence: "This expansion in the estimation related to the variation of the composition may be due to the volatilization of some Manganese during the annealing treatment."

➲ **Response**

Thanks for the comments. The sentence has been rewritten:

Page 5, L12-14: "They showed that all these progression temperatures increase with the ratio (e/a). The values of this report in our work are 8.05 and 8.07, respectively. This increase in (e/a) values may be due to the volatilization of some Manganese during annealing."

Question 7: Page 5, line 10; which parameter of annealing did you mean? Temperature? Time?

➲ **Response**

Thanks for your valuable comment. We have noted the annealing parameter corresponding to the theoretical basis of the martensitic transformation in the following text:

Page 6, L1-3: "The last parameter is the main parameter must be obtained, to get the kinetic transformation of the both alloys. The Kissinger method for non-isothermal change was used to obtain the activation energy. In this case, the temperature of the peak T is utilized to decide the activation energy of two changes since, it has examined that the change was isokinetic ".

Question 8: Page 6, line 10; What is the importance of critical points? You should explain more about your final result.

➲ **Response**

Thanks for this professional suggestion. The details have been added to the revised manuscript.

Pages 7-8: "Figure 5 shows the plot of $Ln(\beta/T^2)$ versus $1/T$. The values of the activation energy E_a for the annealed alloy were determined by the slope of the $Ln(\beta/T^2)$ versus $1/T$ curves. It is clear that there is a remarkable difference in activation energy for various scanning rates. The calculated values E_a are: 259.604 and 12.215 $kJ.mol^{-1}$, respectively. This difference in E_a leads to a dependence of the cooling rate and the activation energy Ea, where the high cooling rates and the low cooling rates correspond to very different activation energies. Meanwhile, over a wide range of rates (5 to 10 $°C.min^{-1}$) between the both previous activation energies, the high values can slowly change to low values. This enables us to deduce that the critical point position ~8 $°C.min^{-1}$, as shown in Figure 5. The kinetics of other alloys with first-order martensitic transformation, for example Cu-Ni-Al [26], Fe-C(N) [27] and Ti–Al–V [28], as well as the ordering transition kinetics in Ni-Mn-Ga [29] have also been widely determined using Kissinger method [30], based on colorimetric results. While, scaling rates are greater than $5°C.min^{-1}$ in the aforementioned literature, limited work has been limited on the rate dependence of activation energy at lower speeds. Fernandez et al. [31] have shown that there seems to be, by all accounts, a critical point related to the slope of the linear curves of $Ln(\beta/T^2)$ with respect to $1/T$, and attributed this phenomenon to evaluated error. In the study of the Ni-Ti shape memory alloy, Hsu et al. [32] have reported that the martensitic substructure could move from coarse twins to fine twins or stacking defects with cooling rates varying from 0.5 to 25 $K.min^{-1}$. In addition, the atomic displacement of the stacking defects in the surface (0 0 1) with a high cooling rate is only a large part of that with a lower cooling rate. Accordingly, the purpose behind the rate

dependence of activation energy in the present investigation could likely be identified with the way that twinning and atomic displacements in the martensitic change process increase significantly at generally low cooling rates, which causes an increase in activation energy important for the progress. The speed of stage interfaces relies upon just the undercooling as the temperature rate abatements to low values [33]. Thusly, fast sample cooling would support a bigger undercooling in a generally short time in examination with cooling gradually, which is in charge of a bigger chemical driving force, and therefore for lower activation energy."

[26] V. Recarte, J.I. Perez-Landazabal, A. Ibarra, M.L. No, J.S. Juan. High temperature β phase decomposition process in a Cu-Al-Ni shape memory alloy. Mater. Sci. Eng. A 378, 238-242 (2004)

[27] Z. Guo, W. Sha, D. Li. Quantification of phase transformation kinetics of 18 wt.% Ni C250 maraging steel. Mater. Sci. Eng. A **373,** 10-20 (2004)

[28] S. Malinov, Z. Guo, W. Sha, A. Wilson. Differential scanning calorimetry study and computer modeling of $\beta \rightarrow \alpha$ phase transformation in a Ti-6Al-4V alloy. Metall. Mater. Trans. A **32,** 879-887 (2001)

[29] V Sanchez-Alarcos, J.I. Perez-Landazabal, V. Recarte, J.A. Rodrıguez-Velamazan, V.A. Chernenko. J. Phys: Condens. Matter **22,** 166001 (2010)

[30] J. Vazquez, P. Villares, R. Jimenez-Garay. A theoretical method for deducing the evolution with time of the fraction crystallized and obtaining the kinetic parameters by DSC, using non-isothermal techniques. J. Alloy. Compd **257,** 259 (1997)

[31] J. Fernandez, A.V. Benedetti, J.M. Guilemany, X.M. Zhang. Thermal stability of the martensitic transformation of Cu-Al-Ni-Mn-Ti. Mat. Sci. Eng. A **438-440,** 723-725 (2006)

[32] T.Y. Hsu. Martensitic transformation and martensite. Beijing: Science (1999)

[33] Z.Q. Kuang, J.X. Zhang, X.H. Zhang, K.F. Liang, P.C.W. Fung. Scaling behaviours in the thermoelastic martensitic transformation of Co. Solid. State. Commun **114,** 231-235 (2000)

General remarks/

- **References are also added** ([26]→ [33]).
- **The quality of all figures has been improved.**

Sincerely Yours.

Dr. T BACHAGA

Dear Sir,

At first, I would like to thank the reviewer for the constructive remarks and the interest discussions offer for our paper. The given questions pushed us to make another bibliography and discovered the interesting result deduced from the effect of annealing condition on martensitic transition of Heusler $Mn_{50}Ni_{42.5}Sn_{7.5}$ alloy. We have considered all your suggestions, which are corrected in the manuscript as following:

Responses for Reviewer 2 Comments

Question 1: "The paper is reasonably written, headline is o.k. The language needs improvement by native speaker."

➲ **Response**

Thank you for your comment. The English language has been improved.

Question 2: "The figures are rather poor in quality in the present manuscript. Should be delivered in better quality if possible."

➲ **Response**

Yes, you are right. The quality of all figures has been improved.

Question 3: "The only critical scientific point is the Kissinger analysis of DSC data. Fig. 5 shows two ranges, 2 and 5K/min and the data 10K/min and higher heating rate. Corresponding activation energies differ largely. However, if one looks into the original DSC Data fig. 4 it is obvious, that measurements at intermediate heating rates show no single peak, but double hump like structure. Thus, two transformations occur nearly simultaneously. Thus the Kissinger analysis is not directly applicable. Authors need to check and discuss this."

➲ **Response**

Thank you for this professional suggestion. Yes, you are right, if we look at the original DSC data (Figure 4), it is obvious that the measurements at intermediate cooling rates show no single peak, but a double-hump structure. What is unique in our study of the $Mn_{50}Ni_{42.5}Sn_{7.5}$ sample is that two exothermic peaks can be observed during the intermediate cooling rates. Previous studies had never reported such an abnormal phenomenon. They proposed that, in addition to martensitic transformation, another inter-martensitic transformation takes place between two martensitic phases of different structures. Thus, it is reasonable to consider the current transformation peaks in the DSC curve of the $Mn_{50}Ni_{42.5}Sn_{7.5}$ sample as a martensitic transformation and an inter-martensitic transformation, which are completely reversible and reproducible. Furthermore, the purpose of calculating the activation energy is to determine level of energy required by the sample as the martensite transformation takes place, which indicates how stable a structure is displayed by alloy. The Johnson–Mehl–Avrami (JMA) equation for solid state transformation can be used to determine activation energy of shape memory alloys when phase transformations occur. The JMA equation can be applied non-isothermal case. The Kissinger method is proposed for analyzing non-isothermal activation energy of samples. The details have been added to the revised manuscript.

Pages 6-8: "From measurements obtained by DSC, we can examine the theory of martensitic transformation; specifically the activation energy E_a. The last parameter is the main parameter must be obtained, to get the kinetic transformation of the both alloys. The Kissinger method for non-isothermal change was used to obtain the activation energy. In this case, the temperature of the peak T is utilized to decide the activation energy of two changes since, it has examined that the change was isokinetic.

Distinctive cooling rates running from 2 to 50 °C.min^{-1} were used to make these measurements. Figure 4 shows the thermograms acquired for various cooling rates. It is clear that the transition temperatures decrease with increasing cooling rates and the progress temperatures extend demonstrates a propensity to widen with expanding cooling rate. Moreover, what is unique in our investigation of the $Mn_{50}Ni_{42.5}Sn_{7.5}$ sample is that two exothermic peaks can be observed during intermediate cooling rates. Previous studies had never detailed such an abnormal phenomenon [23, 24]. They proposed that, in addition to martensitic transformation, another inter-martensitic transformation happens between two martensitic phases of various structures. In this way, it is reasonable to consider the current transformation peaks in the DSC curve of the $Mn_{50}Ni_{42.5}Sn_{7.5}$ sample as a martensitic transformation and an inter-martensitic transformation, which are completely reversible and reproducible. According to the data obtained from the DSC curve, the peaks temperatures of the inter-martensitic transformations during cooling intermediate cooling rates 10 and 20°C.min^{-1} are 393 and 391 K, respectively. The thermal activation energies of samples were carried out by DSC with different cooling rates as 2, 5, 10, 20, 30 and 50 °C.min^{-1} (Figure 4). The purpose of calculating the activation energy is to determine level of energy required by the sample during martensitic transformation. The Johnson–Mehl–Avrami (JMA) equation for solid state transformation can be used to determine the activation energy of shape memory alloys as phase transformations occur. The JMA equation can be applied non-isothermal case. The Kissinger method is proposed for the analysis of non-isothermal activation energy of samples [25]. From JMA, the fraction X of the SMA_s after a given time t was indicated by the following equation:

$$X=1-\exp[-(Kt)^n] \quad (1)$$

Where n is the Avrami exponent and K is the effective reaction rate usually assigned Arrhenius temperature dependence:

$$K=K_o\exp(-E_a/RT) \quad (2)$$

The Kissinger method is a one solution of Arrhenius equation. The activation energy can be calculated by applying the following equation according to the Kissinger method.

$$\ln(\beta/T^2)=A-E_a/RT \quad (3)$$

Where E_a is the activation energy, T is the maximum peak temperature of transition, R is the gas constant (8.314 J.mol^{-1}), β is the cooling rate and A is the constant coefficient. Figure 5 shows the plot of $\ln(\beta/T^2)$ versus $1/T$. The values of the activation energy E_a for the annealed alloy were obtained from the slope of the line obtained by plotting $\ln(\beta/T^2)$ versus $1/T$. It is clear that there is a remarkable difference in activation energy for various scanning rates.

The calculated values E_a are: 259.604 and 12.215 kJ.mol^{-1}, respectively. This difference in E_a leads to a dependence of the cooling rate and the activation energy E_a, where the high cooling rates and the low cooling rates correspond to very different activation energies. Meanwhile, over a wide range of rates (5 to 10 °C.min^{-1}) between the both previous activation energies, the high values can slowly change to low values. This enables us to deduce that the critical point position ~8 °C.min^{-1}, as shown in Figure 5. The kinetics of other alloys with first-order martensitic transformation, for example Cu-Ni-Al [26], Fe-C(N) [27] and Ti-Al-V [28], as well as the ordering transition kinetics in the Ni-Mn-Ga alloy [29] were largely determined using Kissinger method [30], based on colorimetric results. While, scaling rates are greater than 5°C.min^{-1} in the previously mentioned literature, limited work has been limited on the rate dependence of activation energy at lower speeds. Fernandez et al. [31] have shown that there seems to be, by all accounts, a critical point related to the slope of the linear curves of Ln(β/T^2) with respect to 1/T, and attributed this phenomenon to evaluated error. In the investigation of the Ni-Ti shape memory alloy, Hsu et al. [32] reported that the martensitic substructure could move from coarse twins to fine twins or stacking defects with cooling rates changing from 0.5 to 25 K.min^{-1}. In addition, the atomic displacement of the stacking defects in the surface (0 0 1) with a high cooling rate is just a large part of that with a lower cooling rate. Therefore, the reason behind the rate dependence of activation energy in the present examination could probably be identified with the way that twinning and atomic displacements in the martensitic transformation process increase significantly at generally low cooling rates, which causes an increase in activation energy important for the progress. The speed of stage interfaces relies upon just the under-cooling as the temperature rate reductions to low values [33]. Thus, the rapid cooling of the samples would promote greater under-cooling in a generally short time during an examination with progressive cooling, which is responsible for a larger chemical driving force, and therefore lower activation energy. In this way, an example of rapid cooling would reinforce greater under-cooling in a relatively short examination time, with step cooling, which is responsible for a greater synthetic main thrust, and along these lines for lower initiation vitality ''.

[23] H.X. Zheng, M.X. Xia, J. Liu, J.G. Li. Martensitic transformation of highly undercooled Ni-Fe-Ga magnetic shape memory alloys. J. Alloy. Compd **385**, 144 (2004)
[24] H.X. Zheng, J. Liu, M.X. Xia, J.G. Li. Martensitic transformation of Ni-Fe-Ga magnetic shape memory alloys. J. Alloy. Compd **387**, 265 (2005)
[25] H. Fang, B. Wong, Y. Bai. Kinetic modelling of thermophysical properties of shape memory alloys during phase transformation. Const. Buil. Mater **131**, 146–155 (2017)
[26] V. Recarte, J.I. Perez-Landazabal, A. Ibarra, M.L. No, J.S. Juan. High temperature β phase decomposition process in a Cu-Al-Ni shape memory alloy. Mater. Sci. Eng. A **378,** 238-242 (2004)
[27] Z. Guo, W. Sha, D. Li. Quantification of phase transformation kinetics of 18 wt.% Ni C250 maraging steel. Mater. Sci. Eng. A **373,** 10-20 (2004)
[28] S. Malinov, Z. Guo, W. Sha, A. Wilson. Differential scanning calorimetry study and computer modeling of $\beta \rightarrow \alpha$ phase transformation in a Ti-6Al-4V alloy. Metall. Mater. Trans. A **32,** 879-887 (2001)

[29] V Sanchez-Alarcos, J.I. Perez-Landazabal, V. Recarte, J.A. Rodrıguez-Velamazan, V.A. Chernenko. J. Phys: Condens. Matter **22,** 166001 (2010)
[30] J. Vazquez, P. Villares, R. Jimenez-Garay. A theoretical method for deducing the evolution with time of the fraction crystallized and obtaining the kinetic parameters by DSC, using non-isothermal techniques. J. Alloy. Compd **257,** 259 (1997)
[31] J. Fernandez, A.V. Benedetti, J.M. Guilemany, X.M. Zhang. Thermal stability of the martensitic transformation of Cu-Al-Ni-Mn-Ti. Mat. Sci. Eng. A **438-440,** 723-725 (2006)
[32] T.Y. Hsu. Martensitic transformation and martensite. Beijing: Science (1999)
[33] Z.Q. Kuang, J.X. Zhang, X.H. Zhang, K.F. Liang, P.C.W. Fung. Scaling behaviours in the thermoelastic martensitic transformation of Co. Solid. State. Commun **114,** 231-235 (2000)

Sincerely Yours.

Dr. T BACHAGA

General remarks/

- **References are also added** ([26]→ [33]).
- **The quality of all figures has been improved.**

Impact of annealing on martensitic transformation of $Mn_{50}Ni_{42.5}Sn_{7.5}$ shape memory alloy

T. Bachaga [1,2, 3*], J. Zhang [1], S Ali [1], J.J. Sunol [3], M. Khitouni [2]

[1] School of Computer Sciences and Technology, University of Qingdao, Qingdao, China.
[2] Laboratory of Inorganic chemistry, UR-11-ES-73, University of Sfax, Sfax 3000, Tunisia.
[3]Dep. de Fisica, Universitat de Girona, Campus Montilivi, Girona 17071, Spain.

Abstract

The impact of annealing on the structural and martensitic transformation of $Mn_{50}Ni_{42.5}Sn_{7.5}$ (at.%) shape memory alloy was systematically investigated using a scanning electron microscope (SEM), X-ray diffraction (XRD), and differential scanning calorimetry (DSC). According to XRD studies, martensite phase a 14M modulated monoclinic structure was detected, at room temperature, for as-cast and annealed alloys. In addition, it has observed that during annealing, the transition temperatures have increased relative to the cast alloy. Also, a high dependence between the cooling rate and activation energy has detected. The more detailed characterization of martensitic transition and account of thermodynamic parameters were examined after annealing.

Keywords: Shape memory alloys; Martensitic Transformation; Phase transition temperatures; Annealing; Martensite phase.

* Corresponding author: Tel.: +18615066169490

E-mail address: bachagatarak@yahoo.fr (T. Bachaga)

1. Introduction

Heusler-based Mn-Ni shape memory alloys have received increasing interest in technological applications, due to their potential functional properties during martensitic transformation (MT). This transition is from a cubic austenitic phase $L2_1$ or B2 at high temperature to a martensitic phase, whose structure can be $L1_0$, 10M and 14M at low temperature [1-4]. Their properties make them of particularly interest for improving of new magnetic actuators, magnetic sensors and refrigerants for attractive refrigeration [5]. The Mn-Ni-Sn system has prospective importance as a shape memory alloy. Recently, researchers have examined the physical properties of Heusler alloys $Mn_{50}Ni_{50-x}Sn_x$ system. Coll et al. [6] showed that this system has a unique austenitic of cubic structure and that it transforms into a martensitic phase of different structures with modulation during cooling. The Heusler $Mn_{50}Ni_{50-x}Sn_x$ alloys showed a large magnetic entropy change [7, 8], a significant exchange bias field [9], and a slight thermal delay [10] during the martensitic change. Lately, important reports on the effect of annealing on similar alloys have been distributed. Schagel et al. [11] investigated the effect of annealing on the martensitic phase transformation temperatures in $Ni_{50}Mn_{50-x}Sn_x$ alloys at different cooling rates. The effect of annealing on the martensitic transformation of $Ni_{44.1}Mn_{44.2}Sn_{11.7}$ ribbons was examined by Xuan et al. [12]. They showed that with different annealing temperatures, the MT of the annealed ribbons increases obviously. On the other hand, Fichtner et al. [13] announced that the annealing of alloys resulted in a decrease in martensitic transformation temperatures and an expansion in thermal hysteresis during a martensitic transformation. This could be related to a release of stress during the annealing process. In addition, Liu et al. [14] showed that during an increase in quenching speed of the bulk $Co_{46}Ni_{27}Ga_{27}$ alloy, the martensitic transformation temperature increases monotonically. Also, Sarma et al. [15] found the same correlation for $Co_{47}Ni_{23}Ga_{30}$ ingots. At present, no studies on the effect of annealing on the martensitic transformation of $Mn_{50}Ni_{42.5}Sn_{7.5}$ (at.%) alloy have been performed. Thus, the purpose of this study is to

investigate the impact of annealing on the modification of the microstructure and the behavior of phase transformation temperatures of Heusler $Mn_{50}Ni_{42.5}Sn_{7.5}$ (at.%) alloy.

2. Experimental

An as-cast ingot with a nominal composition of $Mn_{50}Ni_{42.5}Sn_{7.5}$ (at. %) was prepared by arc melting from a Ni metal filament (purity> 99.98%), metallic manganese sheets (purity> 99.98%) and pieces of metallic Sn in the form of small spheres (purity> 99.99%), using Buhler MAM-1 compact arc melting under an argon atmosphere. The mass of the ingot prepared by arc melting was ~ 4 g. An extra 5 wt.% Mn was added to compensate for evaporation losses. The bulk alloy was melted four times, to ensure the homogeneity of the chemical composition. In our case, to better ensure the recycling of the Mn and control the composition, the elements were placed increasingly according to their melting temperatures more precisely the Sn (T_f=231 °C) the lowest and the Mn (T_f=1246 °C) finally the highest Ni (T_f=1455 °C). The bulk alloy was fixed in a quartz tube filled with argon gas, followed by annealing at 1273 K for 1h, and then quenched in ice water. Following that, the obtained samples are named as-cast and annealed. Their microstructures and chemical compositions were determined by scanning electron microscopy (SEM) using a ZEISS DSM-960A microscope operated at 30 kV and linked with an energy dispersive spectrometry (EDX) attachment. The mean grain size was measured from SEM images of as-cast and annealed samples by image J software. The structural characterization of the samples at room temperature (RT) was performed by X-ray diffractometer (XRD), using a Siemens D500 X-ray powder diffractometer with Cu-K_α radiation (λ = 1.5418 Å). XRD refinement analysis was performed by applying Rietveld method and Jana software [16]. The calorimetric measurements were performed by a Mettler–Toledo DSC 822 in a flowing argon atmosphere. DSC curves were determined at different cooling rates, to calculate the activation energy by Kissinger method.

3. Results and discussion

Figure 1 shows the micrographs of as-cast and annealed samples. The granular microstructure of the as-cast ingot is illustrated in Figure 1(a1), where the average grain size of about 1.7 μm are observed. As shown in Figure 1(b1), the grain sizes increased environ 6.6 μm after annealing. It is obvious that the increase in grain sizes after annealing of the alloy. Some EDX measurements were performed on each alloy surface in order to check the homogeneity of the final composition. The standard deviation obtained for the elemental chemical composition (as determined by EDX) was 0.4-0.6 at% for Mn, 0.4-0.6 at% for Ni, and 0.3-0.5 at% for Sn. The EDX analysis of the as-cast and annealed samples is shown in Figure 1(a2) and 1(b2). The results confirm the presence of the metallic mixture. The compositions analysis was found to be in good agreement with the nominal compositions of the as-cast and annealed samples ((49.88 at.% Mn-42.69 at.% Ni-7.43 at.% Sn) and (49.33 at.% Mn-43.22 at.% Ni-7.45 at.% Sn)). The compositions are shifted from the original. It is usual in these alloys obtained by arc melting followed by annealing. To backing the results from the microstructure analysis of both alloys, XRD analysis was performed. X-ray diffraction patterns of the both alloys recorded at room temperature are shown in Figure 2. All the Bragg peaks are sharps and will be indexed as a modulated monoclinic (14M) martensite. The structure of martensite obtained in both alloys is identical to the structure observed in melt spun ribbons with similar composition [4]. It must be remarked that no detected secondary phase could be adjusted to the obtained XRD patterns. The structure of both alloys was almost identical, except for slight differences in the peak intensities and angles, suggesting a decrease in cell volume. The structural parameters are shown in Table 1. Miller indexes were doled out with the guide of ordering programs as Treor and Dicvol. Furthermore, it is seen clear that the diffraction peaks become narrower in both alloys, indicating that the grain sizes of annealed alloy increases, which is consistent with the SEM results. In addition, it should be noted that the diffraction peaks of the samples fade slightly after annealing. This

allows us to deduce that the grain sizes increases after annealing and reduces the Mn-Mn distance. Similar results have found in other Heusler $Ni_{49}Mn_{39}Sn_{12}$ alloys [17].

Figure 3 shows the DSC curves of the as-cast and annealed samples. The characteristic transition temperatures (A_s, A_f, M_s and M_f) are determined. The beginning and end of the transformation temperatures were determined by selecting the intersection of a baseline and the tangents to each peak, as shown in Figure 3. The phase transformation temperatures undergo a slight increase after annealing and the hysteresis width ($\Delta T = A_s - M_f$) shifts from 17 to 25 K, for the annealed sample. The reason for this change can be mainly attributed to the evolution of the atomic ratio of the electron (e/a), the interatomic distance Mn-Mn and the grain sizes. First, as indicated by Krenke et al. [18], the characteristic temperatures of the martensitic transition for the Ni-Mn-Sn system strongly depend on the electron concentration (e/a). They showed that all these progression temperatures increase with the ratio (e/a). The values of this report in our work are 8.05 and 8.07, respectively. This increase in (e/a) values may be due to the volatilization of some Manganese during annealing. Then, as another reason related to this change of martensitic transition temperatures, one can mark the effect of the distance Mn-Mn. Buchelnikov et al. [19] showed that during the rapid solidification from the liquid state to the solid state, the site of the atom in the ingot is too stable and does not take an equilibrium position which it has less than energy. After annealing, the alloy is subjected to a relaxation of the structure, which can slightly modify the site of the atom, causing in the change of the Mn-Mn distance. Finally, another justification for this change is the dependence between the annealing and grain size for annealed alloys observed in micrographs [20-22]. Glezer et al. [22] investigated the correlation between martensitic transition temperatures and grain size in Fe-Ni-B alloys. They noticed that these temperatures decreased with the decrease in grain size and that their critical grain size was smaller than that of the martensitic transformation during cooling.

From measurements obtained by DSC, we can examine the theory of martensitic transformation; specifically the activation energy E_a. The last parameter is the main parameter must be obtained, to get the kinetic transformation of the both alloys. The Kissinger method for non-isothermal change was used to obtain the activation energy. In this case, the temperature of the peak T is utilized to decide the activation energy of two changes since, it has examined that the change was isokinetic.

Distinctive cooling rates running from 2 to 50 °C.min^{-1} were used to make these measurements. Figure 4 shows the thermograms acquired for various cooling rates. It is clear that the transition temperatures decrease with increasing cooling rates and the progress temperatures extend demonstrates a propensity to widen with expanding cooling rate. Moreover, what is unique in our investigation of the $Mn_{50}Ni_{42.5}Sn_{7.5}$ sample is that two exothermic peaks can be observed during intermediate cooling rates. Previous studies had never detailed such an abnormal phenomenon [23, 24]. They proposed that, in addition to martensitic transformation, another inter-martensitic transformation happens between two martensitic phases of various structures. In this way, it is reasonable to consider the current transformation peaks in the DSC curve of the $Mn_{50}Ni_{42.5}Sn_{7.5}$ sample as a martensitic transformation and an inter-martensitic transformation, which are completely reversible and reproducible. According to the data obtained from the DSC curve, the peaks temperatures of the inter-martensitic transformations during cooling intermediate cooling rates 10 and 20°C.min^{-1} are 393 and 391 K, respectively. The thermal activation energies of samples were carried out by DSC with different cooling rates as 2, 5, 10, 20, 30 and 50 °C.min^{-1} (Figure 4). The purpose of calculating the activation energy is to determine level of energy required by the sample during martensitic transformation. The Johnson–Mehl–Avrami (JMA) equation for solid state transformation can be used to determine the activation energy of shape memory alloys as phase transformations occur. The JMA equation can be applied non-isothermal case. The Kissinger method is proposed for the analysis of non-isothermal activation energy of

samples [25]. From JMA, the fraction X of the SMA_s after a given time t was indicated by the following equation:

$$X=1-\exp[-(Kt)^n] \quad (1)$$

Where n is the Avrami exponent and K is the effective reaction rate usually assigned Arrhenius temperature dependence:

$$K=K_o\exp(-E_a/RT) \quad (2)$$

The Kissinger method is a one solution of Arrhenius equation. The activation energy can be calculated by applying the following equation according to the Kissinger method.

$$\mathrm{Ln}(\beta/T^2)=A-E_a/RT \quad (3)$$

Where E_a is the activation energy, T is the maximum peak temperature of transition, R is the gas constant (8.314 $J.mol^{-1}$), β is the cooling rate and A is the constant coefficient. Figure 5 shows the plot of $\mathrm{Ln}(\beta/T^2)$ versus $1/T$. The values of the activation energy E_a for the annealed alloy were obtained from the slope of the line obtained by plotting $\mathrm{Ln}(\beta/T^2)$ versus $1/T$. It is clear that there is a remarkable difference in activation energy for various scanning rates. The calculated values E_a are: 259.604 and 12.215 $kJ.mol^{-1}$, respectively. This difference in E_a leads to a dependence of the cooling rate and the activation energy E_a, where the high cooling rates and the low cooling rates correspond to very different activation energies. Meanwhile, over a wide range of rates (5 to 10 $°C.min^{-1}$) between the both previous activation energies, the high values can slowly change to low values. This enables us to deduce that the critical point position ~8 $°C.min^{-1}$, as shown in Figure 5. The kinetics of other alloys with first-order martensitic transformation, for example Cu-Ni-Al [26], Fe-C(N) [27] and Ti-Al-V [28], as well as the ordering transition kinetics in the Ni-Mn-Ga alloy [29] were largely determined using Kissinger method [30], based on colorimetric results. While, scaling rates are greater than $5°C.min^{-1}$ in the previously mentioned literature, limited work has been limited on the rate dependence of activation energy at lower speeds. Fernandez et al. [31] have shown that there seems to be, by all accounts, a critical point related to the slope of the linear curves of

Ln(β/T^2) with respect to $1/T$, and attributed this phenomenon to evaluated error. In the investigation of the Ni-Ti shape memory alloy, Hsu et al. [32] reported that the martensitic substructure could move from coarse twins to fine twins or stacking defects with cooling rates changing from 0.5 to 25 K.min^{-1}. In addition, the atomic displacement of the stacking defects in the surface (0 0 1) with a high cooling rate is just a large part of that with a lower cooling rate. Therefore, the reason behind the rate dependence of activation energy in the present examination could probably be identified with the way that twinning and atomic displacements in the martensitic transformation process increase significantly at generally low cooling rates, which causes an increase in activation energy important for the progress. The speed of stage interfaces relies upon just the under-cooling as the temperature rate reductions to low values [33]. Thus, the rapid cooling of the samples would promote greater under-cooling in a generally short time during an examination with progressive cooling, which is responsible for a larger chemical driving force, and therefore lower activation energy. In this way, an example of rapid cooling would reinforce greater under-cooling in a relatively short examination time, with step cooling, which is responsible for a greater synthetic main thrust, and along these lines for lower initiation vitality.

4. Conclusions

In summary, the impact of annealing on the microstructure, structural and martensitic transformation of $Mn_{50}Ni_{42.5}Sn_{7.5}$ (at.%) shape memory alloy was studied. On the basis of the experimental results obtained, some conclusions can be cited.

- A martensite phase of a 14M modulated monoclinic structure was detected, at room temperature, for both alloys.
- The phase transformation temperatures increase remarkably after annealing.
- A high dependence between the cooling rates and the activation energy E_a has been detected.

Acknowledgement

This work was funded by the "Taishan Scholar" Project of Shandong Province and Key Basic Research Project of Shandong Natural Science Foundation of China (No. ZR2017ZB0422).

References

1. T. Krenke, E. Duman, M. Acet, E.F.Wassermann, X. Moya, L. Mañosa. Magnetic superelasticity and inverse magnetocaloric effect in Ni-Mn-In. Phys. Rev. B **7575,** 104414 (2007)
2. T. Bachaga, R. Daly, L. Escoda, J.J. Suñol, M. Khitouni. Influence of Chemical Composition on martensitic transformation of MnNiIn Shape Memory Alloys. J. Therm. Anal. Calorim **122,** 167 (2015)
3. J.J. Sunol, L. Escoda, B. Hernando, J.L. Sanchez LIamazares, V.M. Prida. Structural behavior of Ni-Mn-(In, Sn) Heusler melt spun ribbons. J. ESOMAT**,** 02031(2009)
4. T. Bachaga, R. Daly, M. Khitouni, L. Escoda, J. Saurina, J.J. Sunol. Thermal and Structural Analysis of $Mn_{49.3}Ni_{43.7}Sn_{7.0}$ Heusler Alloy Ribbons. Entropy **17,** 646 (2015)
5. G. Yu, Y. Xu, Z. Liu, H. Qiu, Z. Zhu, X. Huang, L. Pan. Recent progress in Heusler-type magnetic shape memory alloys. Rare. Met **34,** 527 (2015)
6. R. Coll, L. Escoda, J. Saurina, J.L. Sanchez-Llamazares, B. Hernando, J.J. Sunol. Martensitic transformation in Mn-Ni-Sn Heusler alloys. J. Therm. Anal. Calorim **99,** 905 (2010)
7. Z. Wu, Z. Liu, H. Yang, Y. Liu, G. Wu. Martensitic and magnetic transformation behaviors in $Mn_{50}Ni_{42-x}Sn_8Co_x$ polycrystalline alloys. J. Phys. D: Appl. Phys **44,** 385403 (2011)
8. A. Ghosh, K. Mandal. Large magnetic entropy change and magnetoresistance associated with a martensitic transition of Mn-rich $Mn_{50.5-x}Ni_{41}Sn_{8.5+x}$ alloys. J. Phys. D: Appl. Phys **46,** 435001 (2013)

9. L. Ma, W.H. Wang, J.B. Lu, J.Q. Li, C.M. Zhen, D.L. Hou, G.H. Wu. Coexistence of reentrant-spin-glass and ferromagnetic martensitic phases in the $Mn_2Ni_{1.6}Sn_{0.4}$ Heusler alloy. Appl. Phys. Lett **99,** 182507 (2011)
10. L. Ma, S.Q. Wang, Y.Z. Li, C.M. Zhen, D.L. Hou, W.H. Wang, J.L. Chen, G.H. Wu. Martensitic and magnetic transformation in $Mn_{50}Ni_{50-x}Sn_x$ ferromagnetic shape memory alloys. J. Appl. Phys **112,** 083902 (2012)
11. D.L. Schlagel, R.W. McCallum, T.A. Lograsso. Influence of solidification microstructure on the magnetic properties of Ni-Mn-Sn Heusler alloys. J. Alloy. Compd **463,** 38 (2008)
12. H. Xuan, K. Xie, D. Wang, Z. Han, C. Zhang, B. Gu, Y. Du. Effect of annealing on the martensitic transformation and magnetocaloric effect in $Ni_{44.1}Mn_{44.2}Sn_{11.7}$ ribbons. Appl. Phys. Lett 92, 242506 (2008)
13. T. Fichtner, C. Wang, A.A. Levin, G. Kreiner, C.S. Mejia, S. Fabbrici, F. Albertini, C. Felser. Effects of Annealing on the Martensitic Transformation of Ni-Based Ferromagnetic Shape Memory Heusler Alloys and Nanoparticles. Metals **5,** 484-503 (2015)
14. J. Liu, M. Xia, Y. Huang, H. Zheng, J. Li. Effect of annealing on the microstructure and martensitic transformation of magnetic shape memory alloys CoNiGa. J. Alloy. Compd **417,** 96 (2006)
15. S. Sarma, A. Srinivasan. Influence of Annealing Temperature on the Properties of Co-Ni-Ga Ferromagnetic Shape Memory Alloy. Adv. Mater. Res **52,** 63 (2008)
16. Petrisek V, Dusek M. Jana. The crystallographic computing system. Institute of Physics: Prague, Czech Republic. (2000)
17. H. Zheng, D. Wu, S. Xue, J. Frenzel, G. Eggeler, Q. Zhai. Martensitic transformation in rapidly solidified Heusler $Ni_{49}Mn_{39}Sn_{12}$ ribbons. Acta. Mater **59,** 5692 (2011)

18. T. Krenke, M. Acet, E.F. Wassermann, X. Moya, L. Manosa. Martensitic transitions and the nature of ferromagnetism in the austenitic and martensitic states of Ni-Mn-Sn alloys. J. Phys. Rev. B **72,** 014412 (2005)

19. V.D. Buchelnikov, S.V. Taskaev, M.A. Zagrebin, A.T. Zayak, T. Takagi. Phase transitions in Ni-Mn-Ga alloys with the account of crystal lattice modulation. J. Mag. Mag. Mater **316,** 591 (2007)

20. T. Sánchez, J.L. Sánchez-Llamazares, B. Hernando, J.D. Santos, M.L. Sánchez, M.J. Pérez, J.J. Suñol, R. Sato, R. Grössinger. Annealing Effect on Martensitic Transformation and Magneto-Structural Properties of Ni-Mn-In Melt Spun Ribbons. Mater. Sci. Forum **635,** 81-87 (2009)

21. M. Kaya, Y. Elerman, I. Dincer. Effect of heat treatment procedure on magnetic and magnetocaloric properties of $Ni_{43}Mn_{46}In_{11}$ melt spun ribbons. Philos. Mag **98,** 1919-1932 (2018)

22. A.M. Glezer, E.N. Blinova, V.A. Pozdnyakov, A.V. Shelyakov. Martensite Transformation in Nanoparticles and Nanomaterials. J. Nanopart. Res **5,** 551-560 (2003)

23. H.X. Zheng, M.X. Xia, J. Liu, J.G. Li. Martensitic transformation of highly undercooled Ni-Fe-Ga magnetic shape memory alloys. J. Alloy. Compd **385**, 144 (2004)

24. H.X. Zheng, J. Liu, M.X. Xia, J.G. Li. Martensitic transformation of Ni-Fe-Ga magnetic shape memory alloys. J. Alloy. Compd **387**, 265 (2005)

25. H. Fang, B. Wong, Y. Bai. Kinetic modelling of thermophysical properties of shape memory alloys during phase transformation. Const. Buil. Mater **131**, 146–155 (2017)

26. V. Recarte, J.I. Perez-Landazabal, A. Ibarra, M.L. No, J.S. Juan. High temperature β phase decomposition process in a Cu-Al-Ni shape memory alloy. Mater. Sci. Eng. A **378,** 238-242 (2004)

27. Z. Guo, W. Sha, D. Li. Quantification of phase transformation kinetics of 18 wt.% Ni C250 maraging steel. Mater. Sci. Eng. A **373,** 10-20 (2004)

28. S. Malinov, Z. Guo, W. Sha, A. Wilson. Differential scanning calorimetry study and computer modeling of β→α phase transformation in a Ti-6Al-4V alloy. Metall. Mater. Trans. A **32,** 879-887 (2001)

29. V Sanchez-Alarcos, J.I. Perez-Landazabal, V. Recarte, J.A. Rodrıguez-Velamazan, V.A. Chernenko. J. Phys: Condens. Matter **22,** 166001 (2010)

30. J. Vazquez, P. Villares, R. Jimenez-Garay. A theoretical method for deducing the evolution with time of the fraction crystallized and obtaining the kinetic parameters by DSC, using non-isothermal techniques. J. Alloy. Compd **257,** 259 (1997)

31. J. Fernandez, A.V. Benedetti, J.M. Guilemany, X.M. Zhang. Thermal stability of the martensitic transformation of Cu-Al-Ni-Mn-Ti. Mat. Sci. Eng. A **438-440,** 723-725 (2006)

32. T.Y. Hsu. Martensitic transformation and martensite. Beijing: Science (1999)

33. Z.Q. Kuang, J.X. Zhang, X.H. Zhang, K.F. Liang, P.C.W. Fung. Scaling behaviours in the thermoelastic martensitic transformation of Co. Solid. State. Commun **114,** 231-235 (2000)

Figures Captions:

Figure 1: Typical SEM micrographs of $Mn_{50}Ni_{42.5}Sn_{7.5}$ alloy: (a) As-cast, (b) Annealed.

Figure 2: The XRD patterns of $Mn_{50}Ni_{42.5}Sn_{7.5}$ alloy: (a) As-cast, (b) Annealed.

Figure 3: DSC curves of $Mn_{50}Ni_{42.5}Sn_{7.5}$ alloy: (a) As-cast, (b) Annealed.

Figure 4: DSC charts of annealed $Mn_{50}Ni_{42.5}Sn_{7.5}$ alloy recorded at different cooling rates.

Figure 5: The $Ln(\beta/T^2)$ vs. $1/T$ plot at different cooling rates of annealed $Mn_{50}Ni_{42.5}Sn_{7.5}$ alloy.

Figure 1

Click here to access/download;Figure;Figure 1.tif

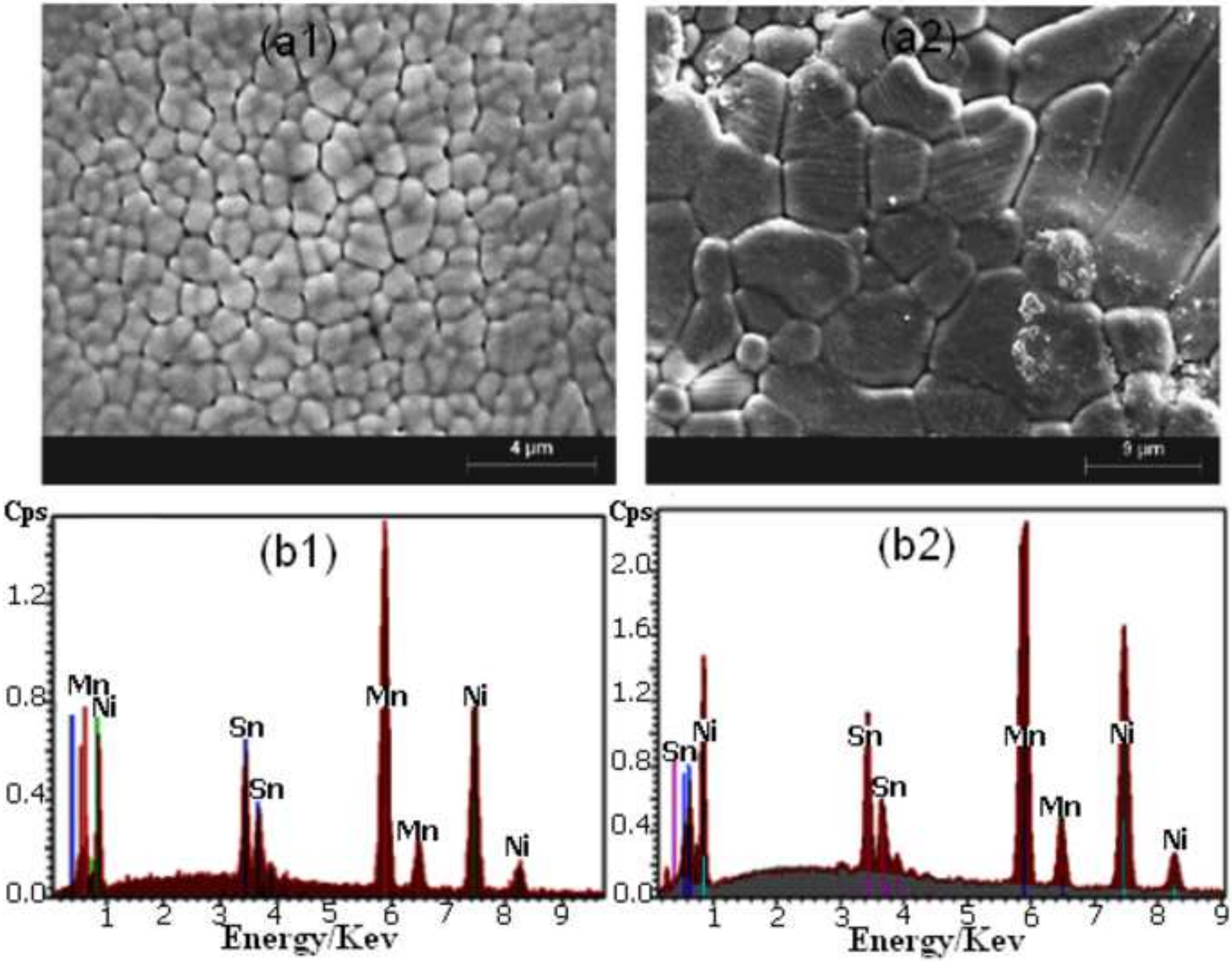

Figure 2

Click here to access/download;Figure;Figure 2.tif

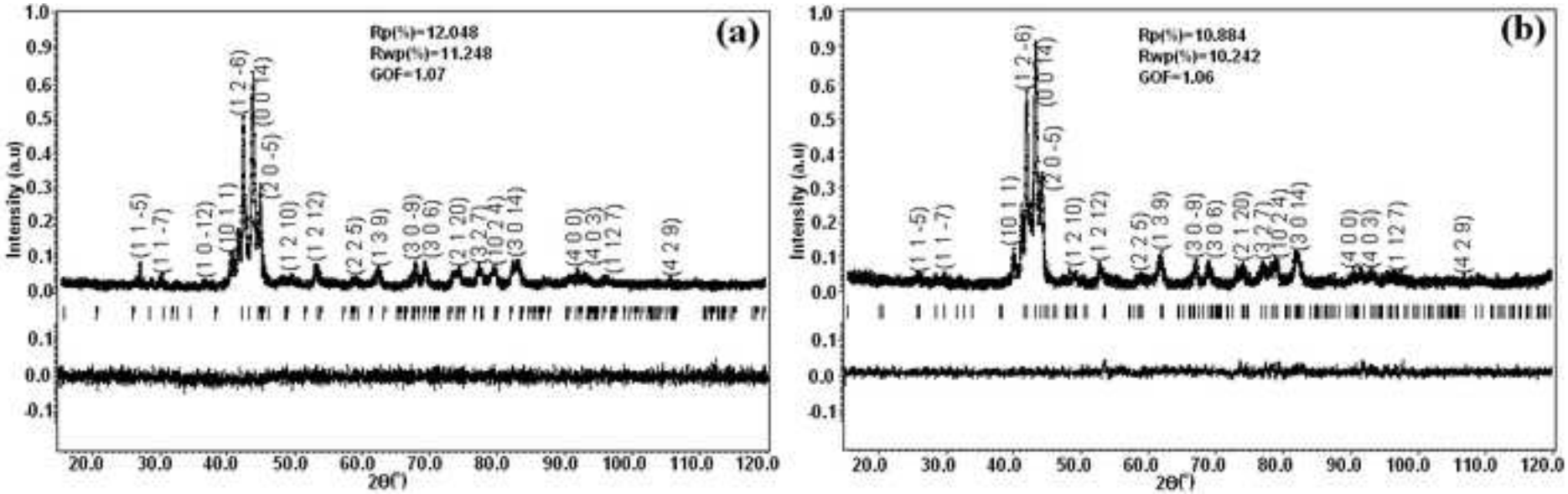

Figure 3

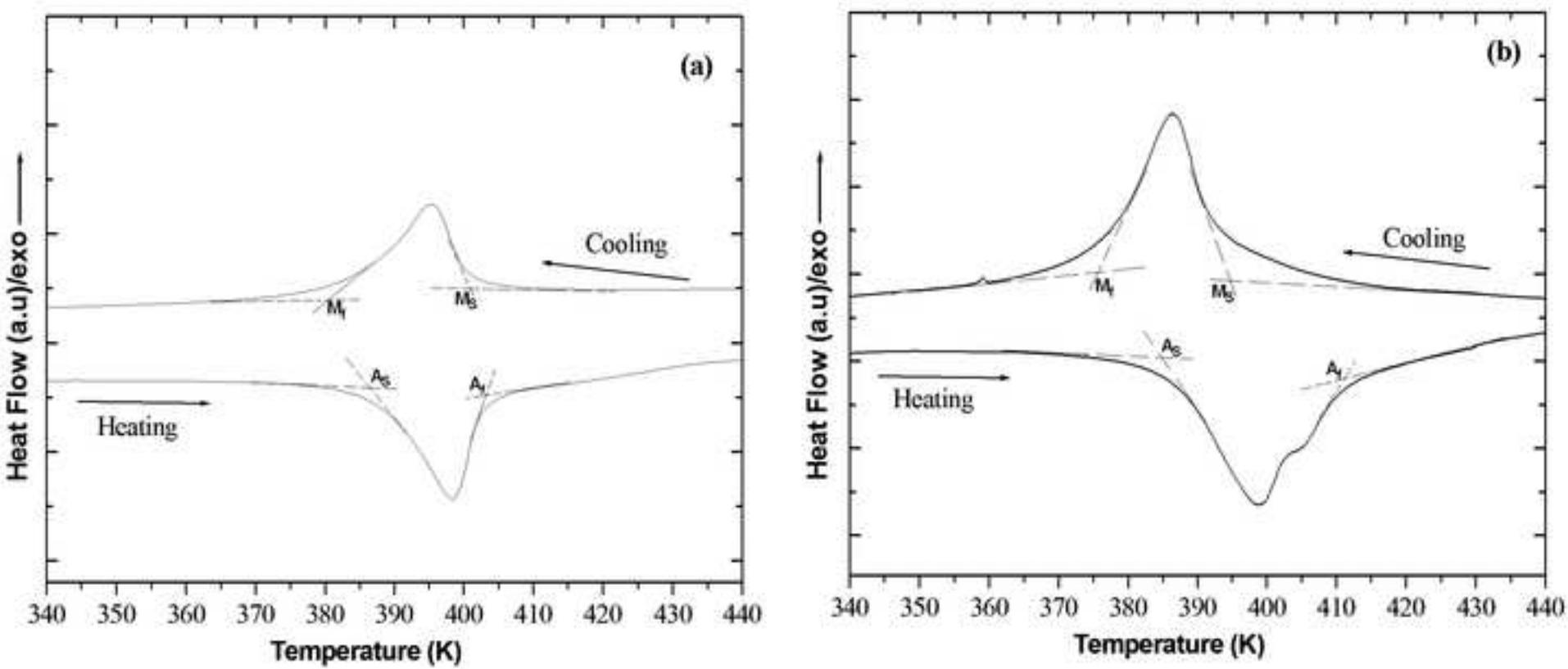

Figure 4

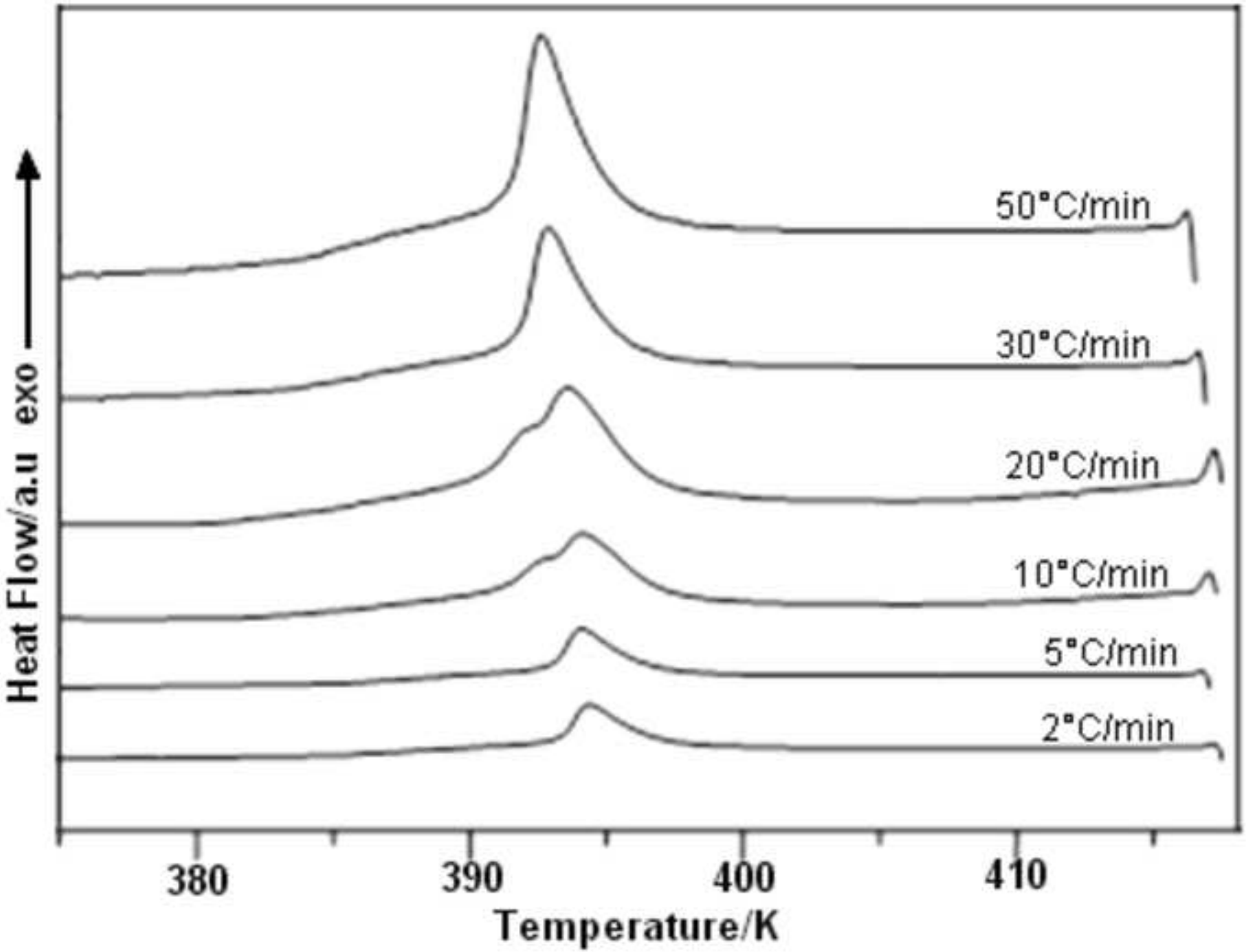

Figure 5

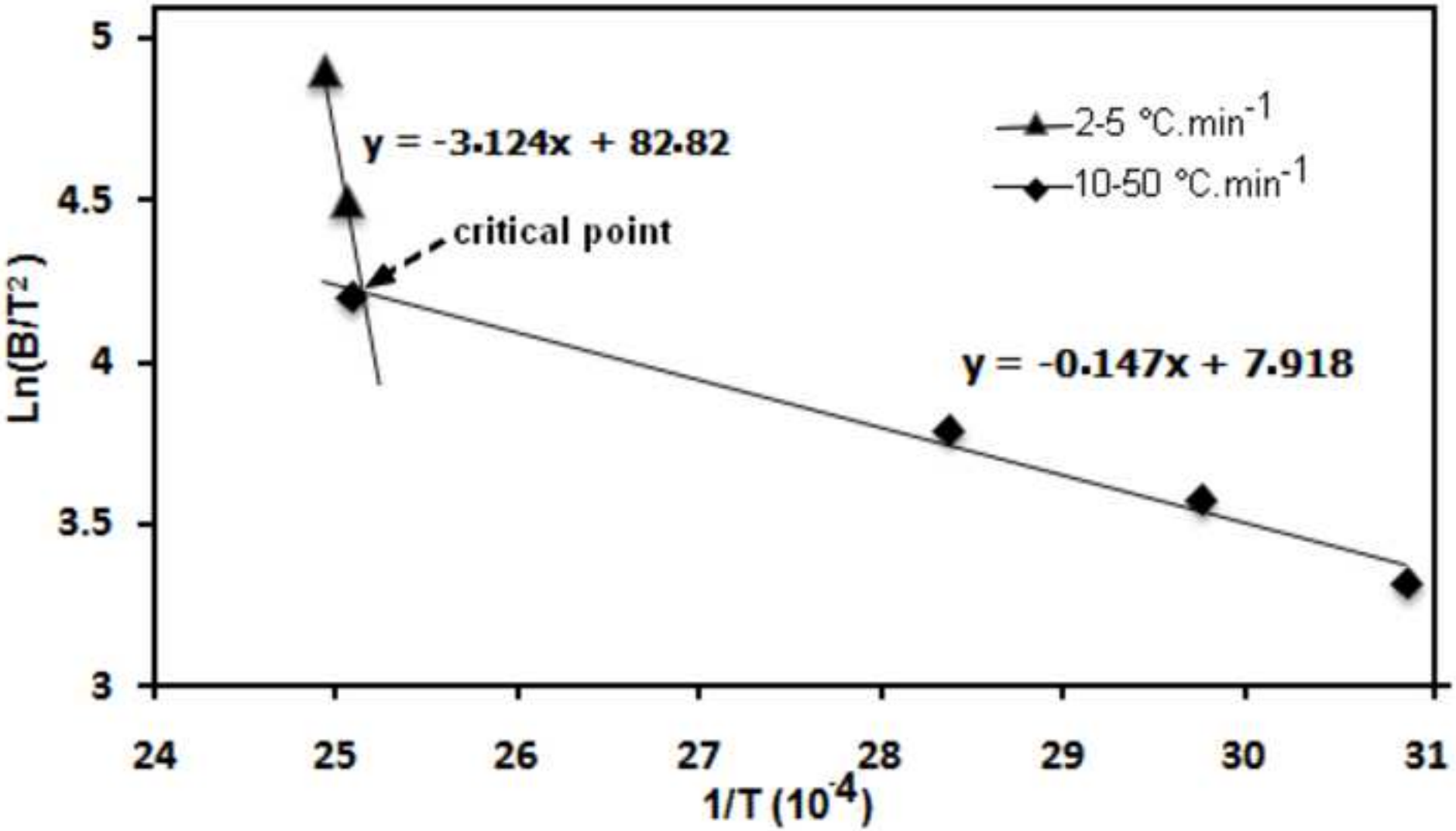

Table 1. Refined unit cell parameters values of Heusler $Mn_{50}Ni_{42.5}Sn_{7.5}$ alloy.

$Mn_{50}Ni_{42.5}Sn_{7.5}$ alloy	**Lattice parameters**				
	a (Å)	**b (Å)**	**c (Å)**	**β(°)**	**Volume ($Å^3$)**
As-cast	4.3196 (3)	5.6109 (3)	29.9216 (2)	93.98	723.45 (2)
Annealed	4.3077 (3)	5.6003 (3)	29.8950 (2)	93.57	719.79 (2)